Received: 8 October 2022 | Accepted: 11 November 2022

DOI: 10.1002/pamm.202200230

# Steep resonance of parametrically excited active MEMS cantilevers for dynamic mode in Atomic Force Microscopy

**Jonathan Ehrmann**[1,*], **Robert Reichert**[1], **Stefanie Gutschmidt**[2], and **Thomas Sattel**[1]

[1] Group of Mechatronics, Technische Universität Ilmenau, Ilmenau, Germany
[2] Department of Mechanical Engineering, University of Canterbury, Christchurch, New Zealand

Ongoing developments in nanotechnology demand higher spatial resolution and thus, higher amplitude sensitivity in Atomic Force Microscopy (AFM). In this work, active cantilevers with integrated sensor and actuator systems are parametrically excited using a novel, analog feedback circuit. With that it is possible to adapt the strength and sign of a cubic nonlinearity which provides a bound to the amplitudes in resonance operation . The system response shows steeper resonance curves and therefore higher amplitude sensitivities compared to forced excited cantilevers. Theoretical findings are validated experimentally.



## 1 Introduction

Nowadays, the ongoing development of live sciences and industrial manufacturing technologies in nanotechnology demands higher spatial resolution for surface topographic analysis. One important technique for such analyses is the Atomic Force Microscope (AFM), which is a subgroup of the so-called Scanning Probe Microscopes (SPM), [1, p. 597]. Generally, the AFM can be distinguished between those using passive probes and the others utilizing active probes, see Fig. 1. The probes itself are structured as micro cantilevers. Shortly, in dynamic mode AFM a micro cantilever is forced excited by a *probe actuator* at a fixed frequency, which is in the vicinity of the cantilever's first bending mode eigenfrequency. The oscillating micro cantilever is moved along the sample surface in x-direction at nanometer distance, see Bhushan [1]. Due to distance depending interaction forces $F_{\mathrm{ts}}(\zeta)$, so-called tip-sample interaction forces, between the cantilever's tip and the surface of the sample, a shift of the eigenfrequency of the coupled probe-sample system occurs, when the distance $\zeta$ between cantilever tip and sample surface changes. Therefore, a change of the micro cantilevers amplitude occurs and is measured. This is illustrated in Fig. 1b). A *z-Scanner* corrects the distance $\zeta$ within a feedback control loop to keep the quasistatic part of it constant. In such a way it is possible to get the topology and other characteristics of the sample.

Passive cantilevers neither have sensors nor actuators included. So, AFM with passive cantilevers needs external sensors and actuators. Usually, the sensor comprises a laser combined with a photo diode. For actuation in most cases a piezoelectric transducer is chosen with base excitation of the cantilever, see Fig. 1. Active cantilevers have both, sensor and actuator, integrated into the structure.

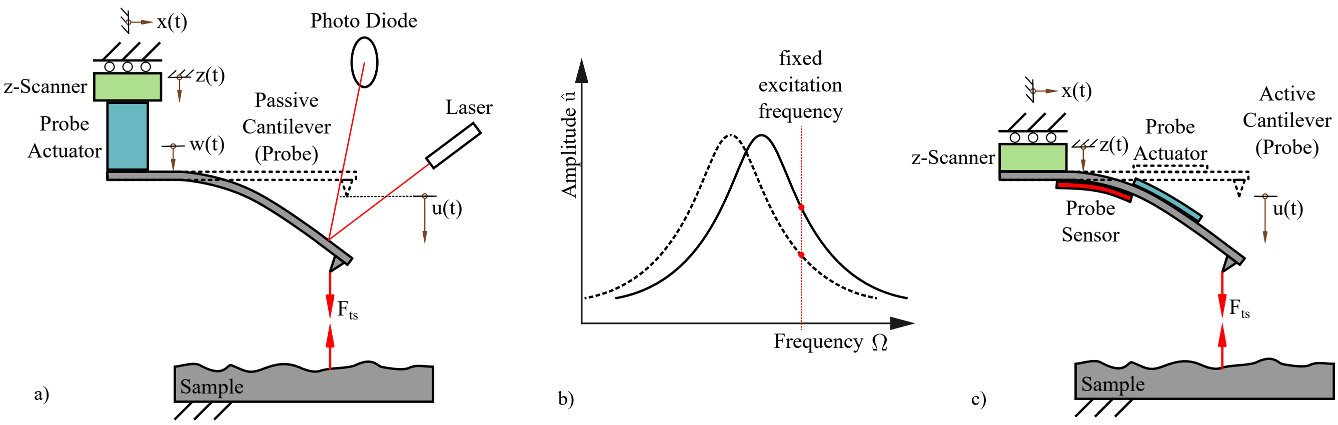


**Fig. 1:** Schematic dynamic mode AFM setups with a probe scanner. With passive cantilever a), with active cantilever c). Shift of eigenfrequency due to tip sample interaction forces b).

In detail, active cantilevers are micro-electromechanical systems, such as those, developed by Rangelow et al. [2] for active SPM. In their work, the sensor system is realised by a piezo-resistive Wheatstone bridge and the actuator system by an electro-thermo-mechanical actuator combined with a bimorph bending structure of the cantilever. An electric current heats up

* Corresponding author: e-mail jonathan.ehrmann@tu-ilmenau.de

the cantilever and the different thermal expansion coefficients of the two bimorph layers cause bending of the cantilever under thermal heating. The thermal heating is realized by an electric current through the aluminum resistor on top of the cantilever. Using a harmonic excitation current results in an oscillating displacement of the cantilever.

Compared to passive cantilevers, active cantilevers offer more compact microscopes with less components. Furthermore, optical alignment of the sensor system (laser and photo diode) and the cantilever itself is not necessary. This has relevance especially when changing the cantilever.

Within AFM, the spatial resolution is determined by the *amplitude sensitivity* of the system that can be understood as the steepness of the resonance curve at the working point (red dot in Fig. 1b, 2a). Now, to increase the amplitude sensitivity of AFM, classical approaches are operating AFM in vacuum [3] or using Q-control [4]. Vacuum leads to a natural increase of the Q-factor and with that steeper resonance curves due to less damping because of air friction. Q-Control uses a feedback circuit to add a controlled, self-exciting effect to the system that artificially increases the Q-factor. So, both approaches lead to higher Q-factors and thus, higher amplitude sensitivity.

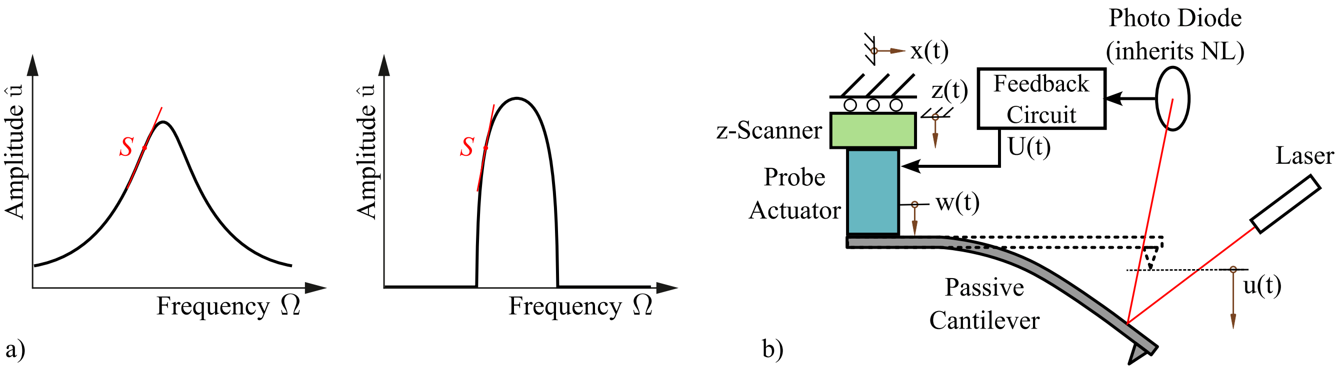


**Fig. 2:** a) Qualitative resonance curves of cantilever (left: forced excitation, right: parametric excitation). b) Feedback circuit as developed by Moreno-Moreno et al. and Prakash et al. [5–7].

Another approach was proposed in a series of works by Moreno-Moreno et al. [5] and Prakash et al. [6, 7]. Their system is schematically illustrated in Fig. 2. To get steeper resonance curves and thus higher amplitude sensitivity, a feedback circuit is used to parametrically excite the cantilever. Parametric excitation means, that one parameter of a system is changed periodically. A classical example is a swing, where the eigenfrequency is modulated by using the own legs to change the length of the swing. The first time parametric excitation was used in the context of cantilevers is the work by Rugar and Grütter, [3].

In the works of Moreno-Moreno and Prakash, parametric excitation is realized as follows. The displacement of the cantilever is read out by a photo diode with an inherent cubic nonlinearity. The signal of the photo diode is fed into the feedback circuit where it is multiplied by a harmonic excitation signal. The output of the feedback circuit is used as input of the actuator. However, the disadvantages of the described system are that first, it includes complex components, i.e., a laser-photo diode sensor system that has to be aligned to the cantilever. This brings disadvantages, as already mentioned above. Second, the functional nonlinearity in the system is not tunable and with it the general frequency response of the cantilever and the limitation of its parametric resonance amplitude is fixed.

The aim of this work is to demonstrate for the first time a novel approach for parametric excitation of active cantilevers in dynamic AFM to achieve higher amplitude sensitivities than with classical forced resonance excitation. The proposed approach utilizes a self-developed analog circuit with parametric excitation and nonlinear displacement amplitude limitation. The nonlinearity is tunable and with that the steepness of the parametric resonance curve is also tunable and can be adapted to the process conditions and sample properties. The basic effects are shown with active cantilevers. The proposed work distinguish from state-of-the art results [5–7] by using a engineered nonlinearity for parametric resonance limitation and not an instrinsic one.

## 2 Theory

Improved sensitivities can be achieved by operating in vacuum [3] and/or applied Q-control modi [4], both with forced excitation. To obtain yet steeper resonance curves and thus higher amplitude sensitivities, parametric excitation is a promising pathway. Prakash et al. [5–7] use a feedback circuit as shown in Fig. 2b to parametrically excite a passive cantilever, which conventionally is base excited as shown in Fig. 1a. The cantilever's equation of motion for the first bending eigenmode is given by the modal lumped mass model

$$m\,\ddot{u} + d\,\dot{u} + k\,u = k\,w(t)\ , \tag{1}$$

 

with the cantilever tip displacement $u(t)$, the base excitation $w(t)$ as well as the modal mass $m$, damping $d$ and stiffness $k$, respectively. For the sake of simplicity, the damping term in excitation neglected.

The *tip-sample force* $F_{\mathrm{ts}}(\zeta)$ is not included there and elsewhere, because it is not necessary for demonstrating the parametric oscillating mechanisms, discussed in this work. Now, in this case, (1), the tip displacement $u(t)$ of the cantilever is read out by a photo diode which inherits a nonlinear behavior, see Fig. 1a). So, the voltage signal $U_{\mathrm{s}}(t)$ of the photo diode is

$$U_{\mathrm{s}} = K_{\mathrm{s}} \left( u + \gamma u^2 + \delta u^3 \right) \ , \tag{2}$$

see [7, p. 5, (6)]. This sensor equation comprise the sensor-displacement proportionality factor $K_{\mathrm{s}}$ and the factors $\gamma$, $\delta$ of the inherent nonlinearities of the photo diode. The signal $U_{\mathrm{s}}(t)$ is then multiplied by a harmonic excitation signal

$$p(t) = \hat{p} \, \cos \varOmega t \, . \tag{3}$$

The resulting signal is fed back to the actuator and yields the equation of motion of the parametrically excited passive cantilever

$$m \, \ddot{u} + d \, \dot{u} + k \left[ (1 + K_{\mathrm{s}} \, p(t)) \, u + K_{\mathrm{s}} \, \gamma \, p(t) \, u^2 + K_{\mathrm{s}} \, \delta \, p(t) \, u^3 \right] = 0 \ . \tag{4}$$

According to the authors [7, p. 6], the cubic term $k \, K_{\mathrm{s}} \, \delta \, p(t) \, u^3$ limits the parametric resonance. It also bends the resonance curve to the left, due to $\delta < 0$, and therefore causes a softening behavior.

The proposed concept by [5–7] leads to a change of the qualitative frequency response of the system from the known behavior of conventional forced excitation to a new behavior of parametric excitation where the resonance curve is steeper and out of the resonance equal to zero, as seen in Fig. 2a. By this, higher amplitude sensitivity is achieved. Unfortunately, the limitation of the resonance and the general frequency response is fix due to the inherent nonlinearity. Also, the nonlinearity is coupled with the parametric excitation. So far, this represents state-of-the-art knowledge.

As mentioned before, the aim of our work is to achieve a design with i) tunable strength of nonlinearity and ii) a nonlinearity which is independent from that parametric excitation, thus avoiding terms $p(t) \cdot u^3$-Term. To keep the explanation simple and to see the governing main effects clearly, a purely phenomenological model of the active cantilever is given here. Alternatively, there exists a model built in our group that models the cantilever as bimorph, electro-thermo-mechanical Euler-Bernoulli beam model, [8]. In this work, it was decided to represent the cantilever as a longitudinal oscillator. In Fig. 3 the model is sketched.

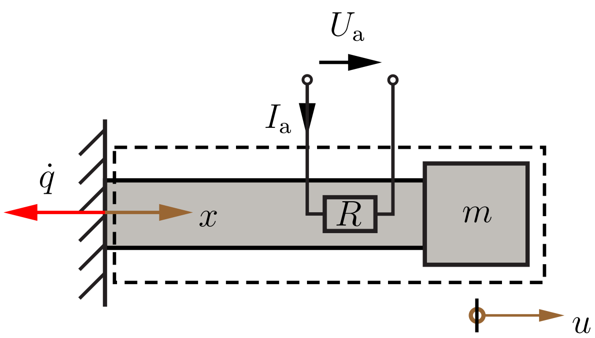


**Fig. 3:** Simple lumped mass modal cantilever model with eletro-thermomechanical actuation.

A massless rod with modal mass $m$ at its end is excited electrically by the voltage $U_{\mathrm{a}}$. Aluminum wires cover the rod surface. The current through the Aluminum wires with Ohmic resistance $R$ results in Joule heating. In our model only heat conduction is represented. Convectional and radiation effects are neglected. The temperature rise then leads to a thermomechanical elongation of the rod. This effect represents the electro-thermomechanical actuator.

The model consists of two dynamic equations, a thermomechanical one and a electrothermal one with the state variables tip displacement and tip temperature difference compared to environment, $(u, \, \theta)$,

$$m\ddot{u} + d\dot{u} + k^{\theta} u = \frac{1}{2} A \tau \, \theta \ , \tag{5}$$

$$\frac{1}{2} m \, c^S \, \dot{\theta} + \lambda \, \frac{A}{l} \, \theta = \frac{1}{R} \, U_{\mathrm{a}}^2(t) \ . \tag{6}$$

The first equation comes from the linear momentum equation of a lumped mass model. The second equation represents one-dimensional heat conduction from the cantilever tip to the apex, where the cantilever is supported. The geometric parameters are the rod length $l$ and the cross section area $A$. The other parameters are the modal mass $m$, the modal damping $d$, the modal stiffness $k^{\theta}$ from the mechanical side as well as the heat capacity $c^S$ and the heat conductivity $\lambda$ from the thermal side. On the right hand sides are the thermal actuation coefficient $\tau$ in the mechanical equation and the Ohmic resistance $R$ of the aluminum heater and the electric actuation voltage $U_{\mathrm{a}}$ in the electrothermal equation.

 

The piezoresistive sensor voltage signal $U_\mathrm{s}(t)$ of the Wheatstone bridge is proportional to the cantilevers tip displacement $u(t)$

$$U_\mathrm{s} = K_\mathrm{s}\, u\,, \tag{7}$$

with the gain of the sensor $K_\mathrm{s}$. Contrary to the optical readout in (2) the piezoresistive readout is linear.

For achieving the design objective a self-developed analog electronic circuit for parametric excitation of active cantilevers was developed. A schematic overview of the developed feedback loop and the cantilever is shown in Fig. 4. The voltage

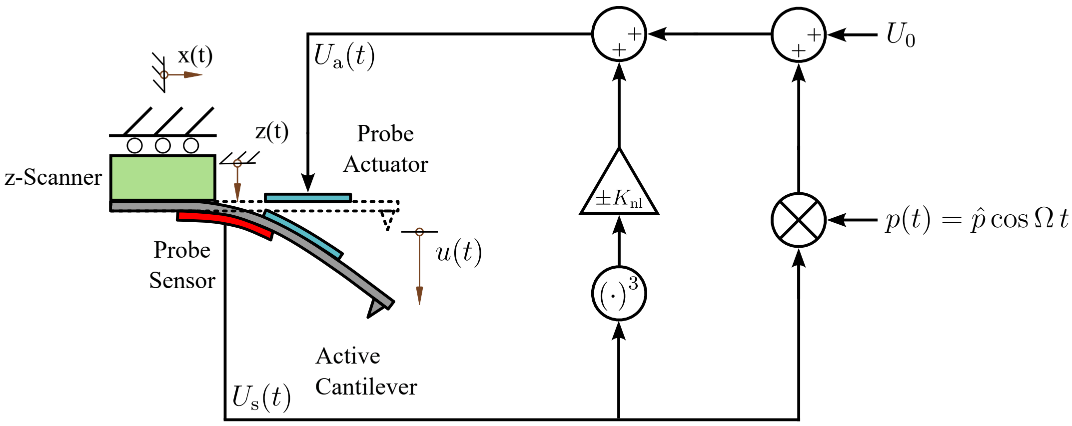


**Fig. 4:** Feedback loop for parametric excitation with cubic resonance limitation. Sensor voltage signal $U_\mathrm{s}$ is processed to get nonlinearity term and by inserting excitation term $p(t)$ and offset $U_0$. The resulting signal $U_\mathrm{a}$ is fed back to the probe actuator.

signal of the piezoresistive sensor $U_\mathrm{s}$ is fed into the circuit, where it is processed in two branches. In the first branch, the signal is multiplied by itself two times to get a cubic nonlinearity term $U_\mathrm{s}^3(t)$ for *parametric resonance limitation*. Afterwards, the cubic term is multiplied by a tunable gain $K_\mathrm{nl}$ to set the sign and strength of the nonlinearity. In the second branch, the signal is multiplied by a harmonic *parametric excitation signal* $p(t) = \hat{p}\cos\Omega t$. After that, an offset voltage $U_0$ is added. To get the excitation voltage signal $U_\mathrm{a}(t)$, both branches are added, so that the parametric modulated, displacement proportional signal together with the cubic nonlinearity gives

$$u_\mathrm{p} = U_0 + p\, U_\mathrm{s} + K_\mathrm{nl}\, U_\mathrm{s}^3\,. \tag{8}$$

Compared to the parametric modulated signal with the passive cantilever contained in (4), here the nonlinearity is separately from the parametric modulation $p$.

This signal $u_\mathrm{p}$ is negative fed back to the proportional controller (P-control), which results in the actuation voltage $U_\mathrm{a}$ of the heater

$$U_\mathrm{a} = K_\mathrm{P}\, e\,, \quad \text{with} \quad K_\mathrm{P} > 0\,. \tag{9}$$

Here $K_\mathrm{P}$ is the controller's proportionality factor and $e$ the control difference between the desired cantilever tip displacement $u_\mathrm{d}$ and the parametric modulated signal $u_\mathrm{p}$,

$$e = u_\mathrm{d} - u_\mathrm{p}\,. \tag{10}$$

The forced excitation term is set to zero, $u_\mathrm{d} = 0$, to give a purely parametrically excited system. Combining the above equations by subsequently inserting (7) - (9) into (1) results into the equations of motion of the parametrically excited active cantilever

$$m\ddot{u} + d\dot{u} + k^\theta u = \frac{1}{2} A\tau\,\theta\,, \tag{11}$$

$$\frac{1}{2} m\, c^S\,\dot{\theta} + \lambda\,\frac{A}{l}\,\theta = \frac{1}{R}\,\left[-K_\mathrm{p}\,\left(U_0 + p\, K_\mathrm{s}\, u + K_\mathrm{nl}\, K_\mathrm{s}^3\, u^3\right)\right]^2\,. \tag{12}$$

The necessity of the offset term $U_0$ can now be seen in (12) on the right hand side of the equation. Expanding the quadratic expression on the right site of (12) gives

$$\left(\ldots + 2\, U_0\, K_\mathrm{p}^2\, K_\mathrm{s}\,\hat{p}\,\cos\Omega t\, u + \ldots\right) \tag{13}$$

It is clear that without an offset term $U_0$ no primary parametric excitation with $\hat{p}\cos\Omega t\, u(t)$ is possible.

 

## 3 Experiment and Simulation

### 3.1 Setup

**Experiment** The experimental setup consists of circuit boards that contain the described feedback loop and general electronics to operate the active cantilever. Also, digital oscilloscopes with built-in signal generators are used to excite and measure the cantilever's oscillations. A laser vibrometer is used to verify the sensor signal of the active cantilever. The active cantilever is described earlier and has an experimentally determined eigenfrequency of $f_0 = 114.4$ kHz.

The frequency response is measured as a stepped frequency sweep. That means that the desired frequency range is discretized. At each frequency step the cantilever is excited and after reaching the stationary state, 1000 periods of the oscillation are recorded. From those time signals the frequency response is calculated.

The cantilever is also excited classically with forced excitation for comparison. For parametric excitation the excitation frequency is around $f_{\text{exc}} = 2\, f_0$ because we want $\Omega/\omega_0 = 2:1$ parametric resonance to operate the cantilever in the first instability tongue which is wider and therefore better to handle in first experiments compared to the other resonances.

**Simulation** The simulation parameters are chosen in a way that the eigenfrequency $f_0$ of the simulation model is also 114.4 kHz and by this the same as the eigenfrequency of the real cantilever. Furthermore, a damping ratio of $D = 8.74 \cdot 10^{-4}$ is taken from the experimental data. That equals a Q-factor of $Q = 572.15$.

For comparison reasons both parametric excitation and forced excitation are investigated. The excitation voltage terms of the parametrically driven cantilever and the forced excited cantilever for the right hand side of (6) are

$$U_{\text{a, par}}(t) = K_{\text{p}} \left(U_0 + p\, K_{\text{s}}\, u + K_{\text{nl}}\, K_{\text{s}}^3\, u^3\right) \,, \tag{14}$$

$$U_{\text{a, for}}(t) = K_{\text{s}} \left[U_0 + \hat{p}\, \cos \Omega t\right] \,, \tag{15}$$

where the parametrically excited equation of motion is already given in (12). Now, by using the numerical integration solver *ode45*, frequency responses of the system are calculated for both excitation types.

### 3.2 Results

In Fig. 5 the amplitude response plot of the cantilever as resulting from the experiments is shown. The amplitudes are

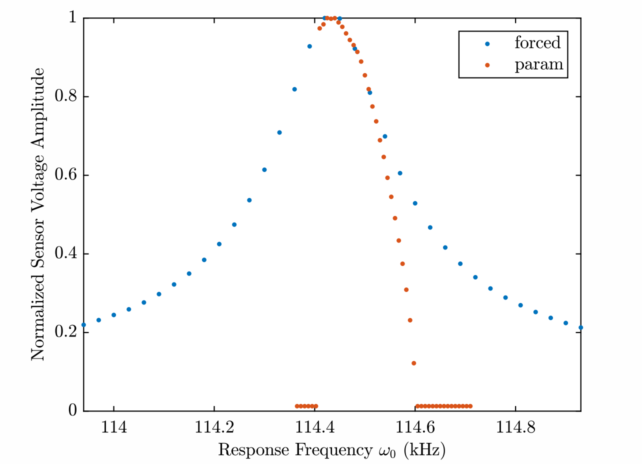


**Fig. 5:** Experimental results comparing classical forced excitation (blue markers) and parametric excitation (orange markers). The latter shows steeper resonance behavior and thus higher amplitude sensitivity.

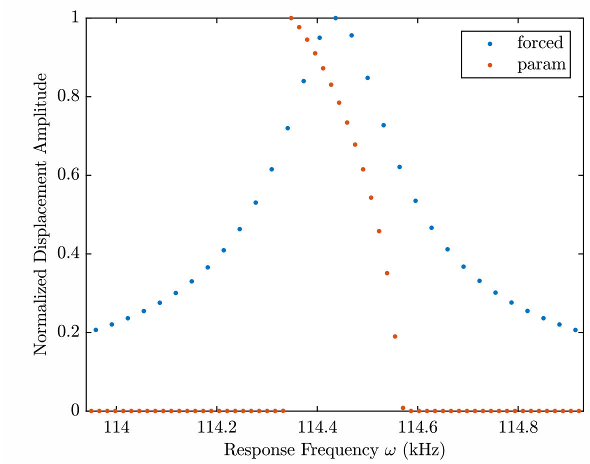


**Fig. 6:** Simulation results show the same qualitatively behavior as experimental results.

normalized by their maximum for better comparison of the general shape of the curves. It is important to note that on the horizontal axis the *response frequency* $\omega$ of the cantilever is plotted and not the excitation frequency $\Omega$. In case of forced excitation, the excitation frequency is identical, $\Omega = \omega$. But in case of parametric excitation the excitation frequency is doubled as mentioned above, $\Omega = 2\omega$. To bring both amplitude response curves in one plot, the response frequency was chosen for all results. Now, comparing both curves it is clear that in the case of parametric excitation the resonance curve is steeper. This yields in higher amplitude sensitivity. The curves bend to the left, showing the softening behavior, which was set by $K_{\text{nl}} < 0$ in the electronics nonlinearity setting.

The result from the simulation can be seen in Fig. 6. Also there, the resonance curve of the parametrically excited system is steeper and equal to zero out of resonance. This is the same qualitative result as in experiment. The detailed shape in the vicinity of the peak is different to the experiment as well as the fact that the peaks of the curves of forced excitation and parametric excitation show a frequency shift to each other. The reason for is not clear yet and could be a result of the modeling itself or some parameter values that are chosen not ideally, i.e. as the strength of the nonlinearity which can not be calculated directly out of the experiment data.

## 4 Conclusion

In this work the theory behind a self-developed analog feedback circuit is shown that enables parametric excitation of active cantilevers for use in dynamic AFM. An experiment and simulation show that it is possible to get steeper resonance curves and with that higher amplitude sensitivity by using the presented system. Smaller discrepancies between experiment and simulation should be investigated in further works.

The proposed approach allows to tune the nonlinearity in the feedback loop to further set the sign and strength of said nonlinearity. Beyond, the nonlinearity is decoupled from the parametric excitation, as is not the case in earlier works, [5–7]. With that, the frequency behavior of the system can be adapt and optimized. This should be investigated in future works by a variation of parametric excitation parameters and nonlinearity parameters for parametric resonance limitation.

**Acknowledgements** The authors would like to acknowledge nano analytik GmbH, Germany, for providing active cantilevers and knowledge in handling them. Open access funding enabled and organized by Projekt DEAL.

## References

[1] B. Bhushan (ed.), Springer Handbook of Nanotechnology (Springer, Berlin, 2007).
[2] I. W. Rangelow, T. Ivanov, A. Ahmad, M. Kaestner, C. Lenk, I. S. Bozchalooi, F. Xia, K. Youcef-Toumi, M. Holz, and A. Reum, Journal of Vacuum Science & Technology B **35**, 06G101 (2017).
[3] D. Rugar and P. Grütter, Phys. Rev. Lett. **67**, 699 (1991).
[4] J. Tamayo, A. D. L. Humphris, R. J. Owen, and M. J. Miles, Biophys. J. **81**, 526 (2001).
[5] M. Moreno-Moreno, A. Raman, J. Gomez-Herrero, and R. Reifenberger, Appl. Phys. Lett. **88**, 193108 (2006).
[6] G. Prakash, S. Hu, A. Raman, and R. Reifenberger, Phys. Rev. B **79**, 094304, (2009).
[7] G. Prakash, A. Raman, J. Rhoads, and R. G. Reifenberger, Rev. Sci. Instrum. **83**, 065109 (2012).
[8] D. Roeser, and S. Gutschmidt, and T. Sattel, and I. W. Rangelow, Journal of Microelectromechanical Systems **25**, 78 (2016).

 